

# Deformation record and revised tectonic evolution of the Nízke Tatry Mts. in the Tatric–Veporic junction area: Insights from structural analysis

KATARÍNA KRIVÁŇOVÁ<sup>1</sup>, RASTISLAV VOJTKO<sup>1</sup>,  
DAVID MILOŠ DROPPA<sup>1</sup> and SILVIA GERÁTOVÁ<sup>1</sup>

<sup>1</sup>Department of Geology and Paleontology, Faculty of Natural Sciences, Comenius University Bratislava, Ilkovičova 6, 842 15 Bratislava, Slovakia;  
✉ [katarina.krivanova@uniba.sk](mailto:katarina.krivanova@uniba.sk), [rastislav.vojtko@uniba.sk](mailto:rastislav.vojtko@uniba.sk), [droppa6@uniba.sk](mailto:droppa6@uniba.sk), [michalikova.silvia@gmail.com](mailto:michalikova.silvia@gmail.com)

(Manuscript received March 20, 2023; accepted in revised form June 14, 2023; Associate Editor: Igor Broska)

**Abstract:** The Nízke Tatry Mts. is a mountain range located in the central part of the Western Carpathians. Throughout history, the studied area has been affected by at least two orogenic cycles – Variscan and Alpine. Based on structural analyses, it is possible to determine several deformation events. The older deformations ( $D^V$ ), which were accompanied by the Variscan higher-grade metamorphism, are characterised by penetrative tectonic foliations, such as schistosity and gneissic banding, and go hand in hand with folds and lineations. In contrast, the younger deformations ( $D^A$ ) are marked by structural evolution under low-grade (retrograde) metamorphism, phyllitic foliations, crenulation foliation, cataclasis, and minor recrystallisation. The Variscan deformation ( $D_2^V$ ) is the earliest pervasive deformation with pronounced evolution of  $S_2^V$  metamorphic foliation, locally with preserved isoclinal and rootless folds of  $S_1^V$  planar fabric. Stretching and mineral lineations ( $L_2^V$ ) are usually oriented in the ENE–WSW direction. The fabric of  $D_2^V$  is intensively affected by folds ( $F_3^V$ ) and, in many places, marked by development of  $S_3^V$  axial planes. The Alpine deformation ( $D_1^A$ ) was accompanied by low-grade metamorphism and depicted by space to zonal with pervasive foliation ( $S_1^A$ ) in some areas. This deformation is characterised by a typical crenulation cleavage, where  $S_2^V$  planes are folded and produced  $S_1^A$  foliation. The crenulation and intersection lineations ( $L_{1c}^A$ ) have NE–SW to E–W trends. The  $D_1^A$  deformation is also accompanied by pronounced evolution of NNW–SSE groove, stretching, and mineral lineation ( $L_{1r}^A$ ). Shortening in the NNW–SSE direction is also evidenced by asymmetric folds with an ENE–WSW orientation of fold axes ( $F_1^A$ ) and line intersections ( $L_{1e}^A$ ) with pronounced top-to-the-NNW tectonic transport. The youngest observed Alpine deformation ( $D_2^A$ ) is related to an extension of the Tatric crystalline basement with top-to-the-east transport defined by Alpine lineations ( $L_2^A$ ) on spaced planar structures ( $S_2^A$ ) and correspond to  $C$  surfaces.

**Keywords:** Central Western Carpathians, Nízke Tatry Mts., Variscan deformation, Alpine deformation, fabric

## Introduction

The Nízke Tatry Mts. is a mountain range that extends into the central part of the Western Carpathians. The Nízke Tatry Mts. is divided into two important sub-units, both from a geomorphological and geological point of view. Their western part contains the Tatric crystalline basement (Ďumbierske Tatry) and their eastern part is composed of the Veporic crystalline basement (Kráľovohorské Tatry). The geographical, as well as the geological boundary of both tectonic units, roughly coincides with the Čertovica shear zone, which can be observed directly on the surface between the villages of Mýto pod Ďumbierom and Nižná Boca through the Čertovica pass (1238 m a.s.l.).

During the Alpine (Cretaceous) tectogenesis, the Tatric Unit was tectonically overlain by the Veporic Unit along this shear zone with an imbricated structure. The study area is bounded by the main ridge of the Nízke Tatry Mts. in the north, by the ridge of Veľký Gápel (1776 m a.s.l.) and the village of Mýto pod Ďumbierom in the south, and by Beňuška (1542 m a.s.l.) in the east.

The geological structure of the crystalline basement and Mesozoic cover sequence has been discussed by several authors in the past (e.g., Zoubek 1936, 1951; Kubíny 1956, 1958, 1960; Siegl 1967, 1970, 1973, 1976a,b, 1981). The structural analysis and reconstruction of deformation phases was performed by Siegl, who described several Variscan and Alpine deformation stages during the seventies and eighties of the twentieth century.

Deformed rocks are one of the most important sources of information available for the observation and reconstruction of the tectonic evolution of the study area. However, observations and interpretations of the geometry of structures in rocks should be used with care. The studied deformed rocks are often the end product of a complex deformation evolution, which means that we can only hope to reconstruct the last deformation stage. Simple geometries, such as folds, foliations, lineations, and boudins can be formed in many ways, and it may seem hopeless to try and reconstruct their evolution from geometrical information only. At any given moment, some degree of misinterpretation of structures is unavoidable and we know that it is a part of the normal process of increa-

sing our understanding of the subject. In this paper, we present the results of a structural geological study showing the main deformation phases during the Variscan and Alpine orogeny, having influenced both the Tatric and Northern Veporic crystalline basements.

### Geological setting

The Western Carpathians form the northeasternmost part of the European Alpine orogenic belt and are traditionally divided into the Internal, Central, and External Western Carpathians (e.g., Andrusov et al. 1973; Plašienka 1999, 2018; Froitzeim et al. 2008). However, some authors also used a simplified model of division into the External and Internal Western Carpathians (e.g., Mišík et al. 1985; Hók et al. 2014). The Central Western Carpathians consist of stacked thick-skinned crustal-scale basement units (Tatric, Veporic, and Gemeric), which are incorporated into the Eo-Alpine collisional wedge and overlying thin-skinned nappes (e.g., Andrusov et al. 1973; Plašienka 1999, 2018; Froitzeim et al., 2008).

The investigated area is located in the central part of the Nízke Tatry Mts., where the pre-Alpine basement is outcropped in the core of the mountains and is overlain by

an Upper Paleozoic–Triassic sedimentary cover or superficial nappes (Fig. 1). The pre-Alpine basement is exposed in both the Tatric and Northern Veporic thick-skinned tectonic units with a polyphase magmatic and metamorphic history that comprises pre-Variscan, Variscan, Permian, and Alpine evolutions (e.g., Matějka & Andrusov 1931; Siegl 1976a, b, 1981; Krist et al. 1992; Bezák et al. 1997; Putiš et al. 1997; Janák et al. 2001; Jeřábek et al. 2008; Plašienka 2018).

The Tatric crystalline basement is composed of two different parts. The northern portion is almost exclusively formed by Upper Devonian to Lower Carboniferous granite to tonalite (Ďumbier- and Prašivá-type with small bodies of leucocratic granite), which were most likely emplaced to the low-grade metamorphosed Klinisko phyllite. In the southern part of the Tatric crystalline basement, a massive complex of intensely-metamorphosed and granitized Lower Paleozoic gneisses, amphibolites, migmatites, and synkinematic Upper Paleozoic granitoids, assigned to the Jarabá Complex (Kamenický in Maheľ et al. 1968) are presented. It is a complex composed of diverse types of rocks that were formed by polystadial metamorphic processes, migmatization, and granitization. In addition to relatively large bodies of the Struhár orthogneiss, synkinematic granites of the Kráľička-type granite, leucocratic granites, and banded paragneiss with amphibolites are encountered together in the complex (Fig. 2).

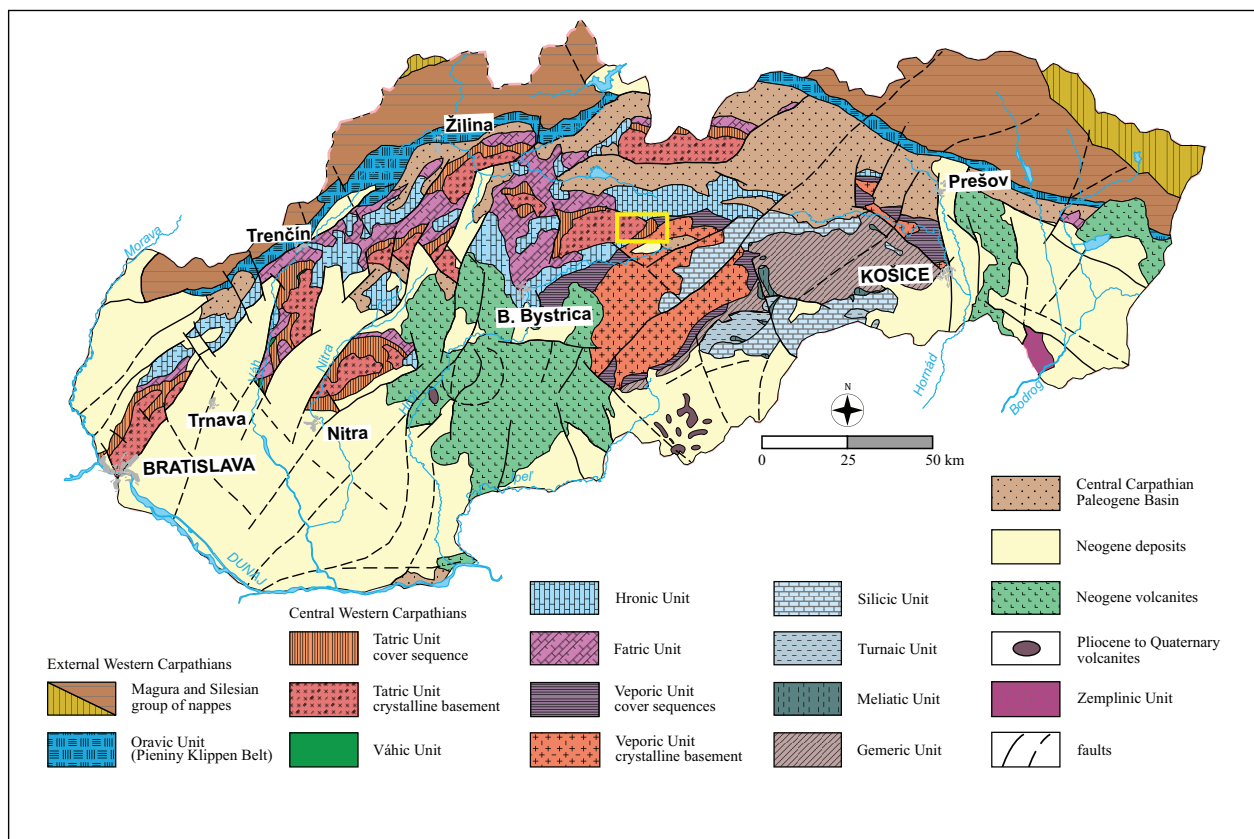


**Fig. 1.** Tectonic map of the Slovak part of the Western Carpathians. The study area is marked by a yellow rectangle (according to Biely et al. 1996).

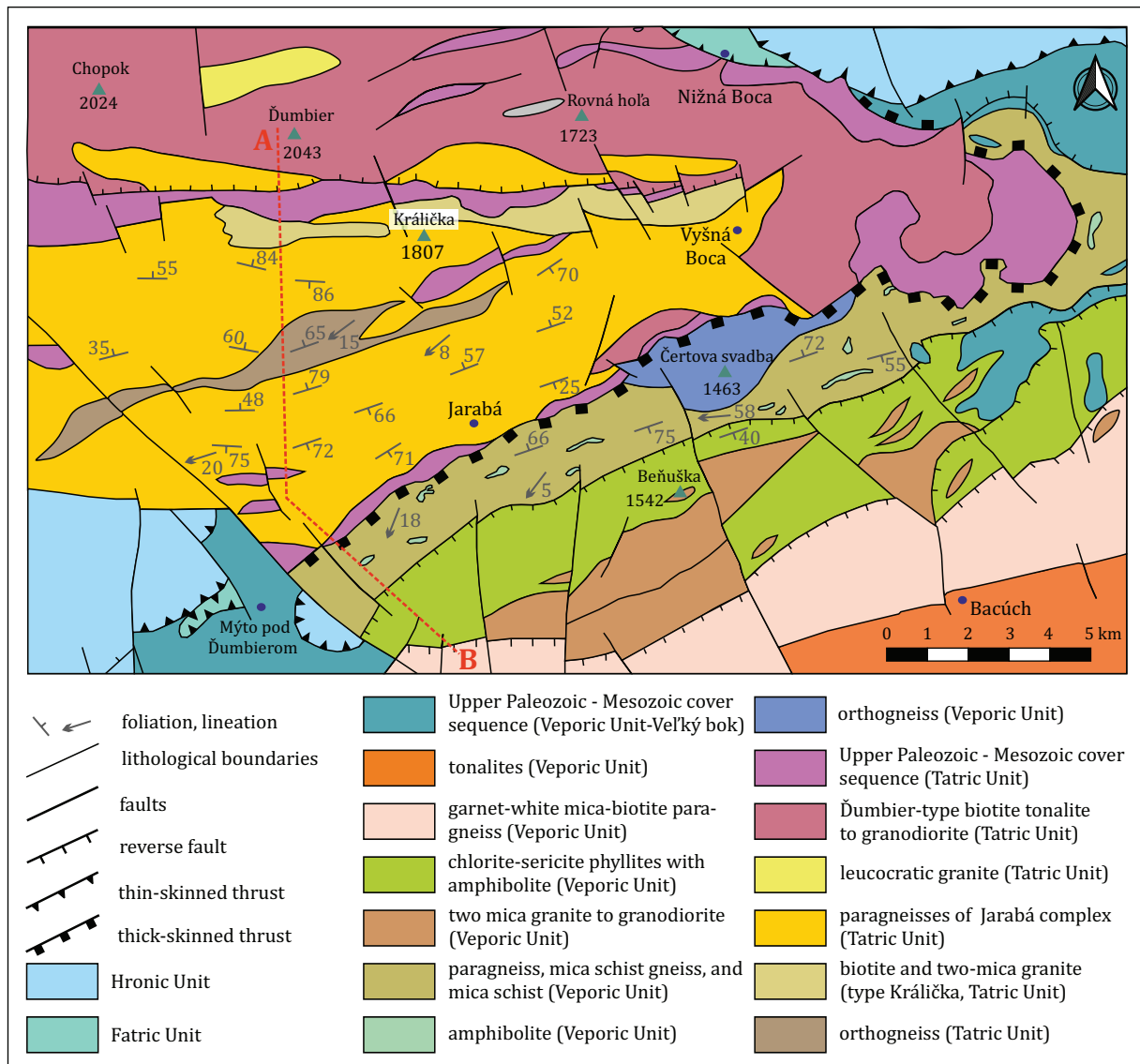


**Fig. 2.** Tectonic map of the study area with Variscan fabric (according to Bezák et al. 2004). Variscan fabric has undergone parallelisation with Alpine fabric (see Fig. 3).

A further, thick-skinned tectonic unit of the Central Western Carpathians, which significantly contributes to the formation of the study area, is the Veporic Unit. This unit was formed during the Eo-Alpine collision and makes up the eastern part of the Nízke Tatry Mts. It is immediately superimposed on the Tatric Unit along the Čertovica shear zone. The Veporic Unit consists of a Lower Paleozoic crystalline basement, which was consolidated during the Variscan orogeny with its Permian–Cretaceous Veľký Bok cover sequence and lies in an autochthonous position relative to the basement (Figs. 2–4).

Recently, three basic lithotectonic units have been distinguished in the Variscan structure of the study area from the bottom to the top (Bezák 1994; Bezák et al. 2004). The lower position is occupied by the middle lithotectonic unit, which is composed mainly of mica schists, gneisses, and remnants of low-grade metamorphites and occurs only in the Veporic

crystalline basement. The middle portion of the basements is composed of the uppermost lithotectonic unit, comprising original, high-grade metamorphosed paragneisses, amphibolites, migmatites, and orthogneisses, which occur mainly in the Ďumbier crystalline basement and the external border of the Veporic basement. The uppermost part of the basement is almost entirely composed of the Ďumbier-type granodiorite to tonalite, which had intruded into the Variscan low-grade metamorphosed complexes.

### Structural record

The study area can be considered well- to very well-exposed, with outcrops often forming distinctive rock cliffs. Nevertheless, the basic, directly-observed structures are only clear in

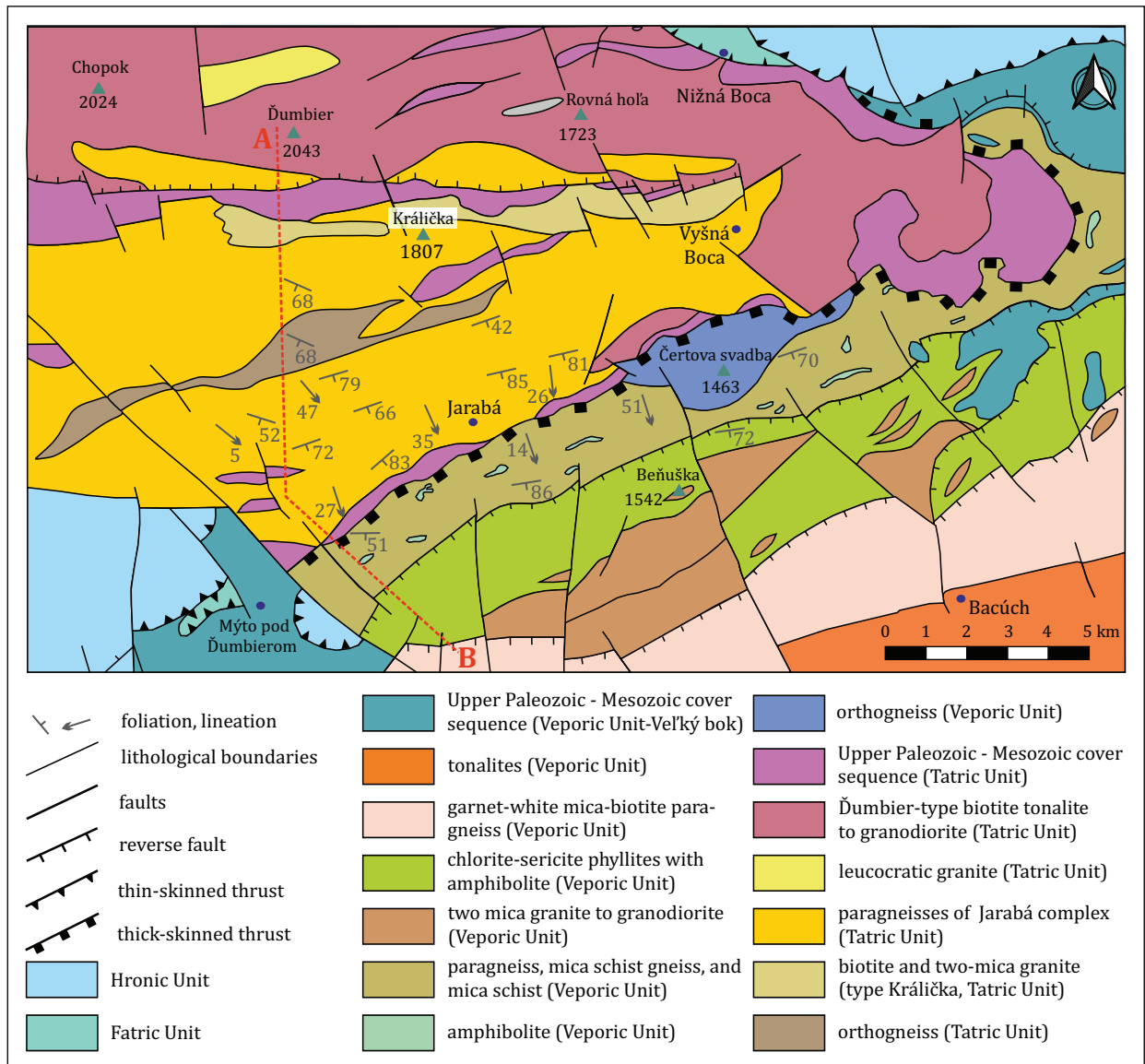


Fig. 3. Tectonic map of the study area with Alpine fabric (according to Bezák et al. 2004).

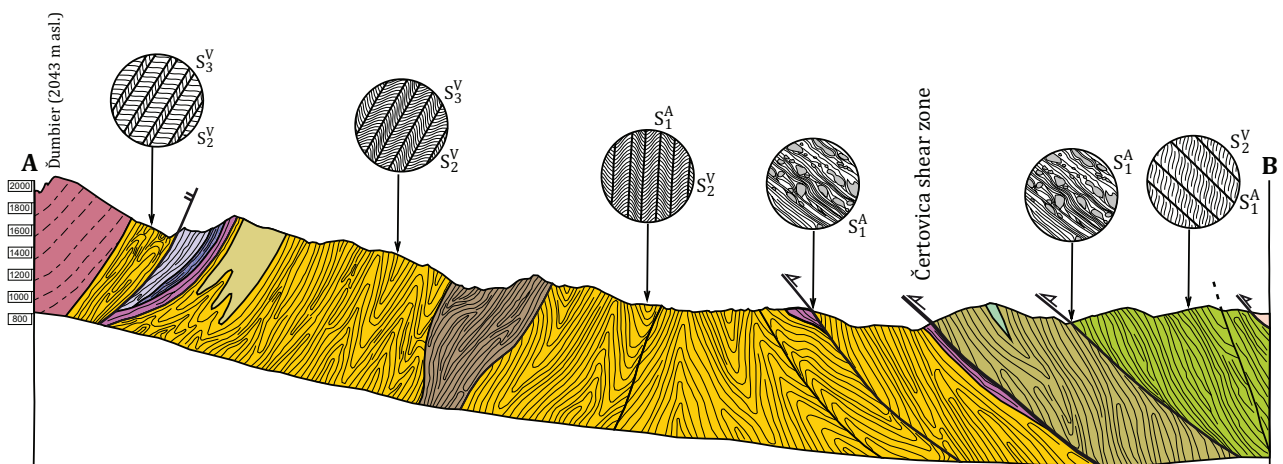


Fig. 4. Geological cross-section through the Tatric and Veporic crystalline complexes. For location of the cross-section see Fig. 2 or Fig. 3.

the domains of the outcrops. The succession of tectonic structures observed in these domains provides the basis for further considerations.

Structural observations were carried out on almost 200 sites covering the area of the Tatric and Veporic units respectively (Figs. 2, 3). The deformational structures were evidenced in the Tatric crystalline basement, Tatric cover sequence, and Veporic crystalline basement.

The orientations of foliation, lineation, fold axial planes, fold hinges, veins, and boudins were collected in the field. The relative or absolute age of deformation was denoted by indexes. It should be noted that any planes (surfaces) are marked as “*S*” with indexes in subscript representing the order of planar structure. For example,  $S_0$  means bedding or magmatic layering (primary planar structure), and  $S_1$  to  $S_n$  represents secondary tectonic foliation. The same classification was also used in the case of linear “*L*” and “*F*” – fold (axes) structures. The linear structures were also divided into parallel with tectonic transport ( $L_t$ ), such as mineral and stretching lineations and perpendicular to the shortening ( $L_c$ ), e.g., an intersection or crenulation lineations. Vector algebra and stereographic projection were employed for the estimation of the orientation of the measured structures (e.g., Ramsay & Huber 1987; Lisle & Leyshon 2004). For the computation of a plane intersection or a plane containing lines, even a plane bisecting two planes, correction of line-plane pairs, and so on, GeolCalc software (developed by R. Vojtko) was used. The visualisation was performed by Stereonet software (developed by R. Allmendinger; cf. Allmendinger et al. 2012; Cardozo & Allmendinger 2013).

The observed and measured mesoscopic, macroscopic, and microscopic tectonic structures were separated into two groups based on what geological units were affected. Those that developed only in the basement were assigned to Variscan, while the others to Alpine ones. The earlier deformation cycle was denoted as  $D^V$  (with a superscript “*V*”) and records Variscan deformation and affects both basements. The latter deformation cycle, which affects both the basements and covers, is related to the Alpine deformation denoted as  $D^A$  (with a superscript “*A*”).

### Variscan structures

The main planar structure of metamorphic rocks is  $S_2^V$  foliation and marked by material inhomogeneity, which originates from the syn-metamorphic crystallisation of rock-forming minerals and their alignment parallel to foliation during the progressive metamorphism (Table 1; Figs. 5, 6). It is the most important pervasive planar structural element of the metamorphosed rocks of the Tatric crystalline basement. The earliest pervasive deformation event ( $D_2^V$ ) produced a high-grade metamorphic schistosity ( $S_2^V$ ) in the paragneiss-mica schist to orthogneiss, locally amphibolite of the Veporic crystalline basement and biotite, as well as two-mica paragneiss, quartz gneiss, sporadically amphibolite, a high-grade orthogneiss fabric, and migmatite layering in the southern part of the

Ďumbier crystalline basement. Formerly, the  $S_2^V$  fabric generally shows E–W strikes (Fig. 2) in the areas unaffected or slightly affected by younger Alpine deformation ( $D^A$ ). Such orientation of the structure is preserved in the southern slopes of Besná and Ďumbier mounts (see Figs. 2, 4). In sporadically-observed localities with preserved bedding planes ( $S_0$ ), the tectonic foliation ( $S_2^V$ ) is mostly parallel. However, parallelism can be a result of the complete transposed primary planes into the  $S_2^V$  pervasive foliation.

It is reasonable to assume that the  $S_2^V$  foliation developed under amphibolite facies conditions was oriented at a high angle to the older planar structures ( $S_1^V$ ). This geometric orientation led to the progressive evolution of tight, isoclinal, and rootless folds. The limbs of the fold are coplanar infinite straight planes that do not intersect at any places with the  $S_2^V$  foliation. It means that the limbs are subparallel to the axial planes (Fig. 5A). In addition, in fine-grained metamorphosed rocks, it is possible to observe relics of small isoclinal folds, which are several centimetres in length ( $F_2^V$ ) and whose limbs are parallel to the pervasive foliation. The orientation of the fold axes ( $F_2^V$ ) varies greatly, but always lies on the foliation surfaces of  $S_2^V$ . This is usually due to different orientations of the incipient fold axis ( $S_1^V$  and  $S_2^V$  intersection) concerning the stretching direction of  $D_2^V$ . So fold axes progressively rotate towards a stretching direction. The axial planes of these tight, isoclinal, intrafolial, and rootless folds or isolated fold hinges are denoted by  $S_1^V$ . For these reasons, the attitude of the  $S_1^V$  foliation is entirely dependent on the orientation of the younger, main, pervasive foliation. Unfortunately, because of the considerable deformation and metamorphism, it is not possible to determine the origin of the  $S_1^V$  foliation (primary structure or an older – pre-Variscan deformation). Nevertheless, this significant planar structure ( $S_2^V$ ) is most likely the result of two geological processes. The first one is likely related to distinctive bedding in original, predominantly-sedimentary rocks, and the second one is related to the noticeable metamorphic differentiation of rock-forming minerals with predisposed older tectonic fabric. However, it can be stated that the metamorphic differentiation caused a change in the grain size of the rock and the presence of minerally-distinct layers with a shrouded connection to the original primary rock. For this reason, we place these deformation structures in the oldest identifiable deformation phase denoted by  $D_1^V$ . No linear structures ( $L_1^V$ ) have been observed that belong to the  $D_1^V$  deformation stage due to strong  $D_2^V$  overprint.

In orthogneisses, the  $S_2^V$  foliation is markedly undulating due to porphyroclasts, possibly in places with a pronounced accumulation of QF-domains (Fig. 5). The QF-domains are composed of feldspar or quartz-feldspar that separate M-domains rich in phyllosilicate minerals (Fig. 6A–D). The porphyroclasts greater than 25 mm are very often rotated, which makes it possible to define the direction of transport. Spatially, the pervasive foliation ( $S_2^V$ ) subtly changes its direction and inclination, which is due to younger, superimposed, predominantly Alpine deformation phases. The stretching and mineral lineations ( $L_{2t}^V$ ) are usually oriented in a NE–SW direction

**Table 1:** Synoptic table of deformational structures (foliations, lineations, and fold axis).

Deformation	Planar fabric	Lineation T	Lineation C/Folds	Tectonic regime	Age
$D_1^V$	$S_1^V$ (E–W)	unknown	various orientation	compression	Early Variscan or older
$D_2^V$	$S_2^V$ (E–W to WSW–ENE)	$L_{2t}^V$ (WSW–ENE)	$L_{2c}^V$ (SW–NE) $F_2^V$ (E–W to SW–NE)	compression	Variscan
$D_3^V$	$S_3^V$ (E–W to WSW–ENE)		$F_3^V$ (E–W to WSW–ENE)	compression	Late Variscan
$D_4^V$	$S_4^V$ (E–W & N–S)			extension	Late Variscan
$D_1^A$	$S_1^A$	$L_{1t}^A$ (NNW–SSE)	$L_{1c}^A$ (WSW–ENE) $F_1^A$ (WSW–ENE)	compression	Eo-Alpine
$D_2^A$	$S_2^A$	$L_{2t}^A$ (WNW–ESE)	$L_{2c}^A$ (NNE–SSW)	extension	Neo-Alpine

(Figs. 2, 6C). The orientation of  $S_2^V$  foliation and  $L_{2t}^V$  lineations in the metamorphic rocks are controlled by the preferred shape of white mica, biotite, amphibole, feldspathic phases, and quartz (Fig. 6).

The  $S_2^V$  foliation is folded by younger non-penetrative folds ( $F_3^V$ ) that occur in banded orthogneisses and migmatites in some places. In general, the trend of fold axes ( $F_3^V$ ) is in an E–W direction with gentle to moderate dip on both sides (Fig. 7D). During this folding,  $S_3^V$  non-penetrative cleavage parallel with fold axial planes of Variscan age progressively developed (Fig. 5C). The  $S_3^V$  cleavage is younger than the main phase of Variscan metamorphism and only local QF-domains mobilization is observed. The orientation of foliation is approximately in an E–W direction. The deformation phase ( $D_3^V$ ) is also characterised by intersection and crenulation lineations, also with a general E–W direction.

Pre-Mesozoic (Variscan) brittle deformation  $D_4^V$  is accompanied by the formation of joints, which were subsequently filled with aplites, pegmatites, or quartz veins ( $S_4^V$ ). The veins are in relatively different directions; however, two directions are significantly dominant:  $S_2^V \parallel S_4^V$  and  $S_2^V \perp S_4^V$ . Observations show that aplite and pegmatite veins predominate in orthogneisses and migmatites, whereas quartz veins, which are often difficult to distinguish from Alpine veins, predominate in biotite paragneisses. No linear structures were observed at this deformation stage (Fig. 7D).

### Alpine structures

The Alpine  $D_1^A$  deformation was accompanied by low-grade metamorphism (lower greenschist facies), mylonitisation, and cataclasis. This deformation ( $D_1^A$ ) is depicted by space to zonal and in some places pervasive foliation ( $S_1^A$ ). The Alpine foliation ( $S_1^A$ ) can be visually identified especially in domains where the newly-formed foliation ( $S_1^A$ ) was oriented at a greater angle (40–70°) to the pervasive Variscan foliation ( $S_2^V$ ). In such domains, asymmetric crenulation cleavage was predominantly formed, where older planes are ( $S_2^V$ ) and newly formed planes represent  $S_1^A$  foliation. In the case of subparallel shortening concerning  $S_2^V$  pervasive foliation, a crenulation foliation ( $S_1^A$ ) was developed (Fig. 8A). This crenulation foliation is often symmetrical, however, in the vicinity of more

intensely-deformed rocks, it becomes asymmetrical with a transport top-to-the-NNW direction. The crenulation and intersection lineations ( $L_{1c}^A$ ) have NE–SW to E–W trends (Fig. 8D). The  $D_1^A$  deformation is also accompanied by pronounced evolution of stretching, and to a lesser extent, mineral lineation represented by orientation of the mean vector  $L_{1t}^A$  156/35° (Fig. 8C). The mineral lineation ( $L_{1t}^A$ ) is formed predominantly by oriented chlorite, quartz, less epidote, and albite aggregates ( $L_{1t}^A$ ) that are oriented in a NNW–SSE direction. Moreover, the attitude of the intersection lineation ( $L_{1c}^A$ ) between the  $S_2^V$  and  $S_1^A$  foliations together with the orientation of fold axes ( $F_1^A$ ) is 245/05° (Fig. 8B). The spatial orientation and geometric relationships of the basic planar and linear structures define the transport of the Alpine thrusting/folding top-to-the-NNW direction.

The general attitude of the poles of Alpine foliation is  $S_1^A$  338/30° (Fig. 8A) on both tectonic units. An interesting feature of  $S_1^A$  foliation is that they tend to parallel the  $S_2^V$  pervasive foliation in the southeastern parts of the study area (Northern Veporic Unit). The occurrence of conformal or dis-conformal transposition is dependent on the spatial orientation of the Variscan foliation during Alpine deformation.

On a map scale, the Alpine structure is characterised by individual inverse/thrust shear zones (Figs. 3, 4). The shear zones are composed of mylonites ( $S_1^A$ ) of predominantly intermediate SE inclination with pronounced internal asymmetry (Fig. 6B, E, F). The sense of shearing in the macroscale was identified by the geometrical relationships of mylonitic foliation and asymmetric crenulation cleavage. In these shear zones, the Variscan pervasive  $S_2^V$  fabric was significantly folded, transposed, and overprinted by the  $S_1^A$  foliation (Fig. 9A, C, D). The sense of shear can also be determined from asymmetrically deformed objects, such as quartz lenses and asymmetry of macro-folds. The results of the geometrical analysis of these indicators, stretching, and mineral lineations, as well as on a microscale refer to top-to-the-NNW transport (Fig. 3). Quartz veins with sulphide, siderite, and precious stone mineralisation have often been observed within these mylonite zones.

In the metamorphosed rocks of the Jarabá Complex of the Tatric Unit and the Northern Veporic Unit, folds ( $F_1^A$ ) of different amplitude and wavelength are presented, which are

genetically distinct from the Variscan  $F_1^V$  and  $F_2^V$  folds (Fig. 7C). Their attitude is like one of Variscan folds (E–W to NE–SW striking of fold hinges), but the inclination of their axial planes is mainly steep to the south and less to the north. Moreover, the inclination of fold axial planes ( $F_1^A$ ) to the southeast is progressively becoming shallower. In addition, the folds southeastward increase their asymmetry, especially in the broader area along the Čertovica shear zone. The folds ( $F_1^A$ ) were more frequently observed in paragneisses and the Mesozoic rock of the cover sequences. In many places, Mesozoic sedimentary tectonic lenses are folded along the

mylonite zones and thus incorporated into the crystalline basement (Bezák & Olšavský 2008). The relatively varied types of folds ( $F_1^A$ ) are conditioned by the rheology of the rocks, the low degree of Alpine metamorphism, and the pronounced planar predisposition of the rocks with pervasive  $S_2^V$  fabric.

The most significant Alpine structure in the Tatric Unit of regional extent is the E–W striking Trangoška synform, which is more than 12 km long. It is formed by Triassic to Jurassic sedimentary rocks, which are considered to be the cover of the Tatric crystalline basement (Fig. 3). The synform has now

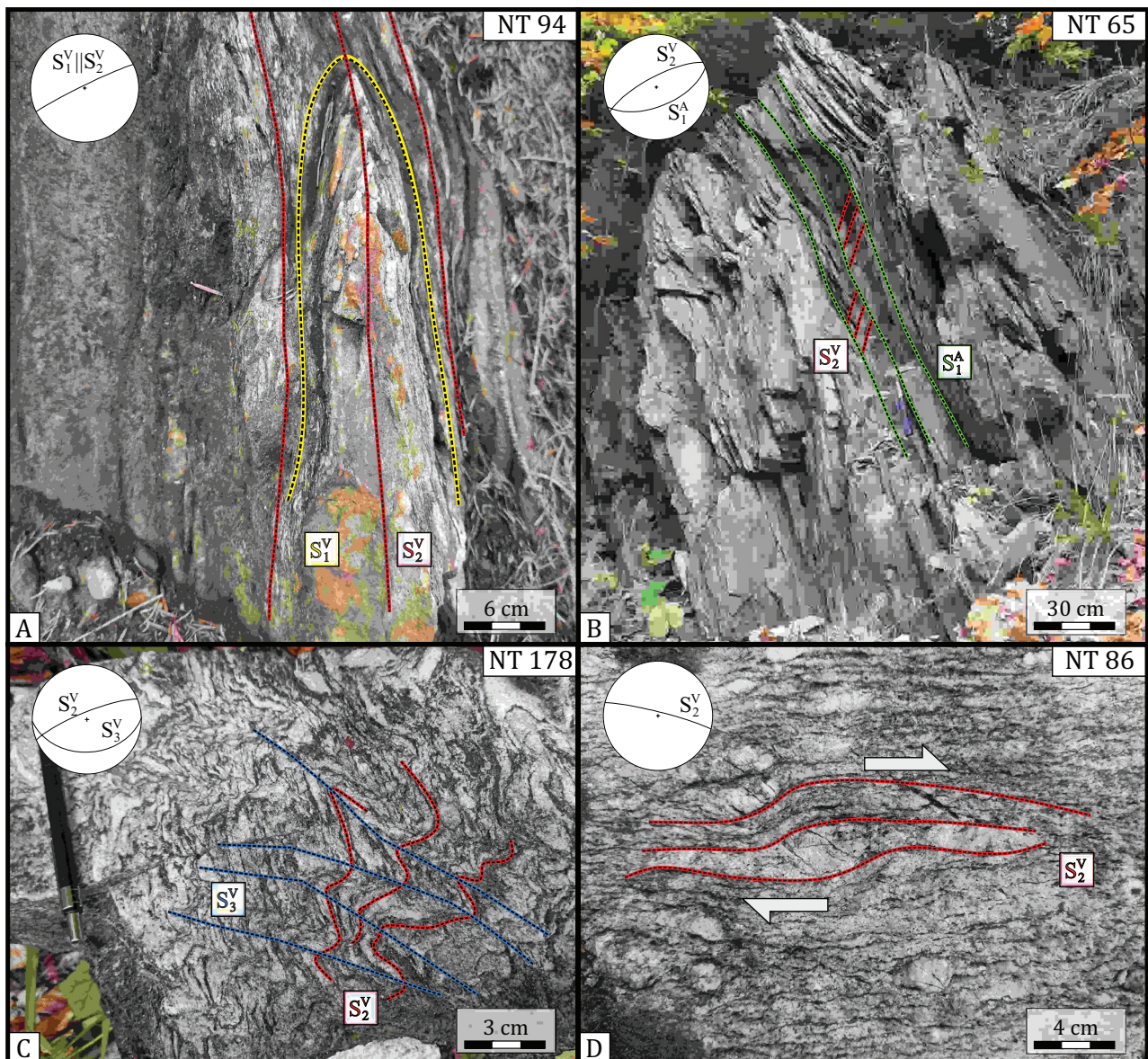


**Fig. 5.** Field photographs of the Variscan fabric: **A** — folded  $S_1^V$  foliation to isoclinal folds with parallel limb to  $S_2^V$  pervasive foliation biotite-bearing paragneiss (Jarabá Complex, Tatric Unit); **B** — partially-preserved Variscan  $S_2^V$  overprinted by pervasive  $S_1^A$  foliations (Hron Complex, Veporic Unit); **C** — folded  $S_2^V$  Variscan foliation with the evolution of  $F_2^V$  folds and  $S_3^V$  cleavage in strongly deformed orthogneiss (Jarabá Complex, Tatric Unit); **D** — Variscan pervasive foliation ( $S_2^V$ ) in porphyric orthogneiss. Porphyroclasts are formed by feldspar or quartz–feldspar forming QF-domains and M-domains are represented by biotite (Jarabá Complex, Tatric Unit). The porphyroclasts asymmetries consistently indicate a top-to-the-SW sense of shear.

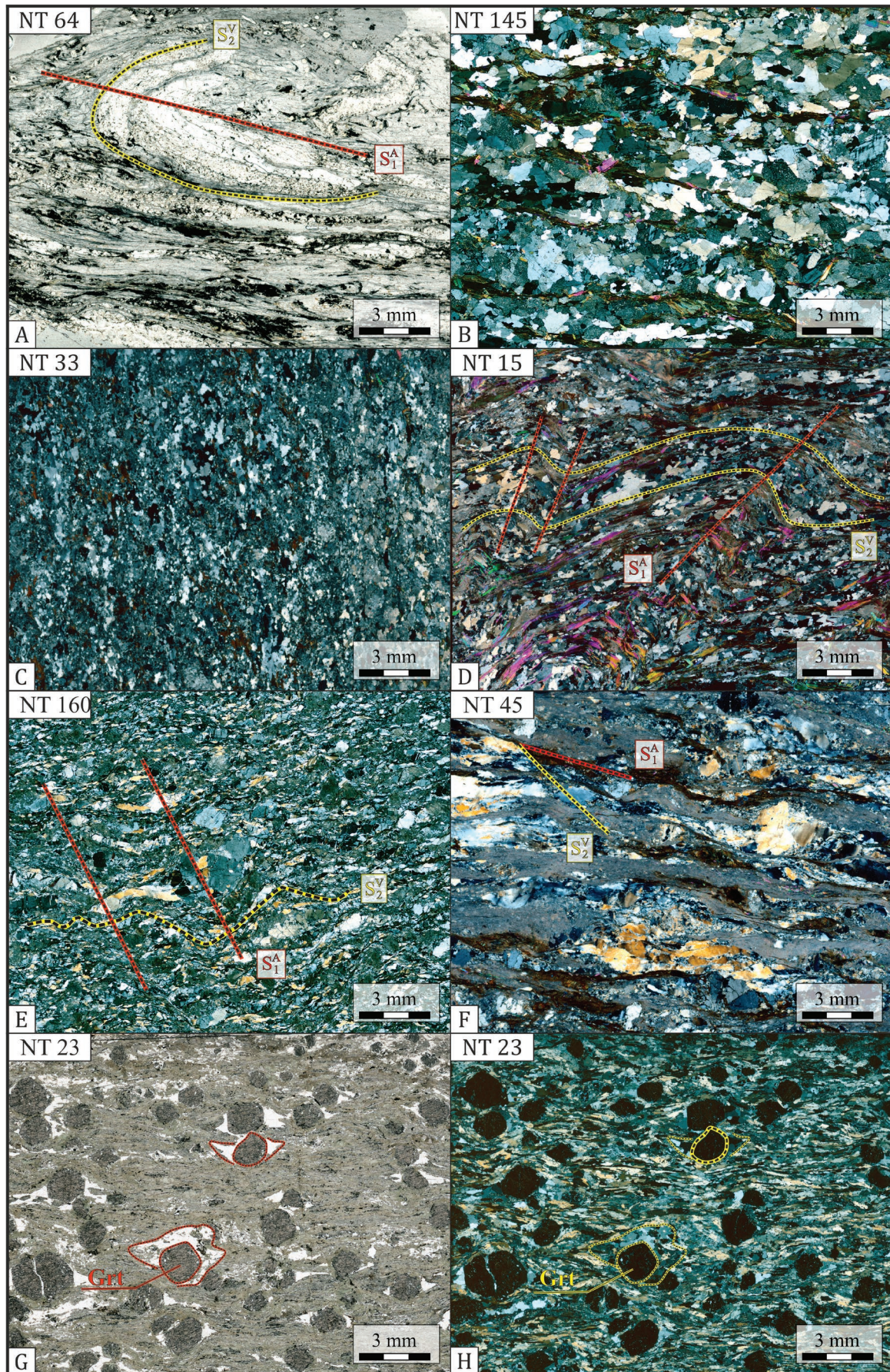




**Fig. 6.** Micrographs of main Variscan and Alpine fabrics: **A** — pervasive Variscan metamorphic foliation ( $S_2^V$ ) with preserved isoclinal folded older  $S_1^V$  foliation in mylonitic gneiss (Hron Complex, Veporic Unit) (PPL); **B** — Variscan pervasive metamorphic foliation ( $S_2^V$ ) in the Jarabá Complex orthogneiss (XPL); **C** — dynamically-recrystallized quartz in an ultramylonite sample; subgrains and recrystallized zones contain small, more equant grains with relatively uniform extinction. The preferred orientation of quartz grains forms the pervasive Variscan foliation ( $S_2^V$ ) (PPL); **D, E** — asymmetric Alpine crenulation cleavage ( $S_1^A$ ), folded foliation is  $S_2^A$  (XPL); **F** — Mylonitic foliation, generally a spaced foliation composed of alternating layers and lenses with different mineral composition or grain size, in which more or less strongly-deformed porphyroclasts are embedded and the mylonitic foliation wraps around these porphyroclasts. In this low- to medium-grade mylonites, quartz ribbons are strongly elongated and show strong undulose extinction and dynamic recrystallisation (XPL); **G, H** — garnet amphibolite-gneiss with Alpine  $S-C$  fabric (G-PPL) and (H-XPL). Note: PPL – plane-polarized light, XPL – crossed polarized light.

truncated the north limb by a northward dipping and E–W striking inverse fault.

The second, less significant Alpine deformation ( $D_2^A$ ) is associated with an extensional tectonic regime (Fig. 9B). It has been observed mainly in Triassic siliciclastic deposits, as well as in the Veporic crystalline basement. Extensional structures, such as en-echelon veins ( $S_2^A$ ), shear zones, and stretching lineation ( $L_{21}^A$ ) refer to top-to-the-east transport. The  $D_2^A$  structures are not pervasive and are localised into the discrete shear zones along the broader area of the Čertovica shear zone.

### Interpretation and discussion

The studied crystalline rock was formed by stress as a function of time, structural level, and deformation properties. The structure of the crystalline basement is complex; it is not distinct at all scales or individual parts due to the inhomogeneity of the deformation phases. Based on the presence of Mesozoic sediments, their deformation, and the different  $p-T$  conditions during metamorphism in the crystalline basement, it is possible to distinguish Variscan ( $D^V$ ) and Alpine deformations ( $D^A$ ).

Four main deformation phases were identified in the Variscan basement of the Tatric and partly-identified in the Veporic crystalline basements, while two were identified in the Permian to Lower Triassic cover. The earliest deformation event denoted as  $D_1^V$  records Early Variscan or pre-Variscan deformation and affects only the Tatric basement; however, it has not been identified in the Veporic crystalline basement yet. Still, we cannot rule it out, and structural observations point to an older deformation than the main Variscan  $D_2^V$  deformation. This deformation ( $D_2^V$ ) has produced a high-grade metamorphic schistosity in the paragneisses-mica schists, as well as a high-grade gneissic banding and migmatite layering of the Jarabá Complex in the Tatric Unit and the basement of the Veporic Unit.

The metamorphosed rocks of the Tatric crystalline basement (Jarabá Complex) are composed of paragneisses with the parageneses of rock-forming minerals (Qz+Pl+Bt+Mu+Gr±Sil), and these rocks can be designated as garnet–sillimanite–muscovite–biotite gneiss that belong to the sillimanite zone (amphibolite facies). The estimated temperature of progressive metamorphism is between 550 to 690 °C, and the pres-

sure varies from 4 to 4.7 kbar (e.g., Krist et al. 1992; Petrik et al. 2006).

The timing of deformations is related to the age of deformed rocks, degree of metamorphism, age of granitoid rocks in the neighbourhood, and the Mesozoic cover sequences. The monazite dating of orthogneiss has also shown a record of two old events (cores vs. overgrown and/or rims). The main phase of metamorphism and strong Variscan reworking, including partial melting, was dated back to the ages between 340–350 Ma (Petrik et al. 2006) and is structurally related to the Variscan deformation ( $D_2^V$ ). However, the data, which gives a range between 380–440 Ma, may be reminiscent of older processes ( $D_1^V$ ). The well-defined, old cores (ca. 480 Ma) found in one orthogneiss sample are, at present, too scarce to give a solid basis for a primary Ordovician age of the orthogneisses, although this possibility cannot be entirely dismissed (Petrik et al. 2006; Putiš et al. 2008).

In the intensively-strained domains of orthogneisses, macroscopically-recognizable  $\delta$ - and  $\sigma$ -type rotated and aligned feldspar porphyroclasts enclosed in dynamically-recrystallized QF- and M-domains. Shape asymmetries of porphyroclasts and alignment of QF-materials around the porphyroclasts, together with mica fishes of biotite flakes, refer to a top-to-the-south ductile thrusting ( $S_2^A$ ). The southern transport of the Variscan nappes was also evidenced by structural analyses from the western part of the Jarabá Complex (e.g., Putiš 1992; Fritz et al. 1992; Madarás et al. 1999; Putiš et al. 2003, 2008).

The granitoid pluton in the northern part of the crystalline basement is composed of the Ďumbier-type granodiorite to tonalite in the study area and was considered to be Variscan in the past (Kantor 1959, 1961; Bojko et al. 1974; Bagdasarjan et al. 1985). More recent data have confirmed the Variscan age using several geochronological methods: Rb/Sr whole rocks 368±22 Ma (Cambel et al. 1990); zircon SIMS U–Th–Pb dating 356±2 Ma (Broska et al. 2013); zircon SHRIMP U–Th–Pb 340±3 Ma (Kohút & Larionov 2021), respectively 353.4±2.2 Ma for the Ďumbier-type tonalite and 352±3.0 Ma for the Prašivá-type granodiorite; (Maraszewska et al. 2022). However, a recent geochronological study from samples taken near the top of Chopok Mt. indicates Early Ordovician (476.8±1.7 Ma) age for the Ďumbier-type granodiorite (a.k.a. Chopok-type granodiorite, according to Burda et al. 2020). Nevertheless, it should be noted that the Early Ordovician age does not make sense, considering the Variscan metamorphism,

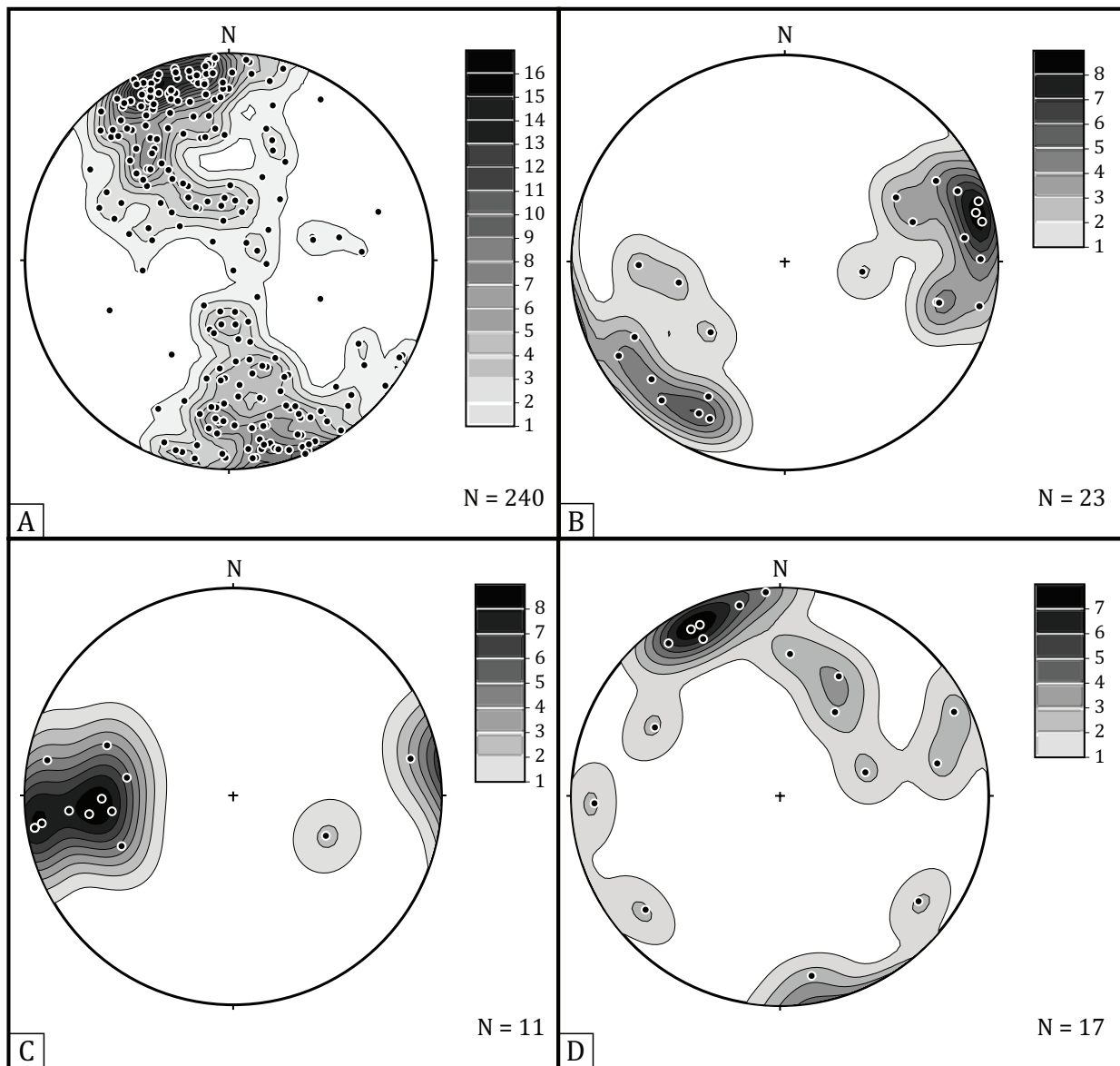


**Fig. 7.** Contour plots of measured Variscan foliation and lineations (Kamb contours in standard deviations, Kamb 1959): **A** — Partially-preserved Variscan  $S_1^V$  and pervasive  $S_2^V$  metamorphic foliations (poles of planes); **B** — Variscan mineral and stretching lineations ( $L_{2c}^V$ ); **C** — Variscan crenulation and intersection lineations ( $L_{2c}^V$ ); **D** — Variscan quartz, aplite, and pegmatite veins ( $S_4^V$ ), presented by poles of planes.

deformation, and knowledge of the structural pattern of basement rocks. Numerous papers point to the spatial association of the Ďumbier-type granodiorite with metamorphosed rocks and do not consider their contact as a thrust surface nor as a host rock for the emplacement of granodiorite intrusions (Kubín 1956, 1958; Siegel 1970, 1976b; Krist et al. 1992; Madarás et al. 1999). The pluton can be characterised as a late-synkinematic, macro- and microscopically anisotropic granodiorite to tonalite body emplaced to the Klinisko phyllite. The internal planar structure is conformal with the Variscan  $S_3^V$  foliation, and of course Alpine deformation ( $D_1^A$ ) was also observed. It is represented by spaced foliation and mylonite zones ( $S_1^A$ ). Most foliations of post-crystalline deformation originated simultaneously and later, most of the faults and

joints as well. The geometry of the Variscan and Alpine deformation was similar, and one part of the structure is overprinted conformly. The shape and the fabric of the pluton developed principally by the Alpine deformation ( $D_1^A$ ).

Nevertheless, the Early Ordovician age of the granodiorite published by Burda et al. (2020) may indicate that granitoids converged with the Jarabá Complex much later, perhaps as late as during the Eo-Alpine convergence. Of course, we cannot exclude that assimilated parts of older granitoid intrusions or orthogneiss (like Králička-type granitic rocks) in the Ďumbier-type granodiorite have been dated. This conjecture requires careful work for the future.

The Variscan tectogenesis had an S-vergence, which means that the thick-skinned crystalline basement thrust sheets were

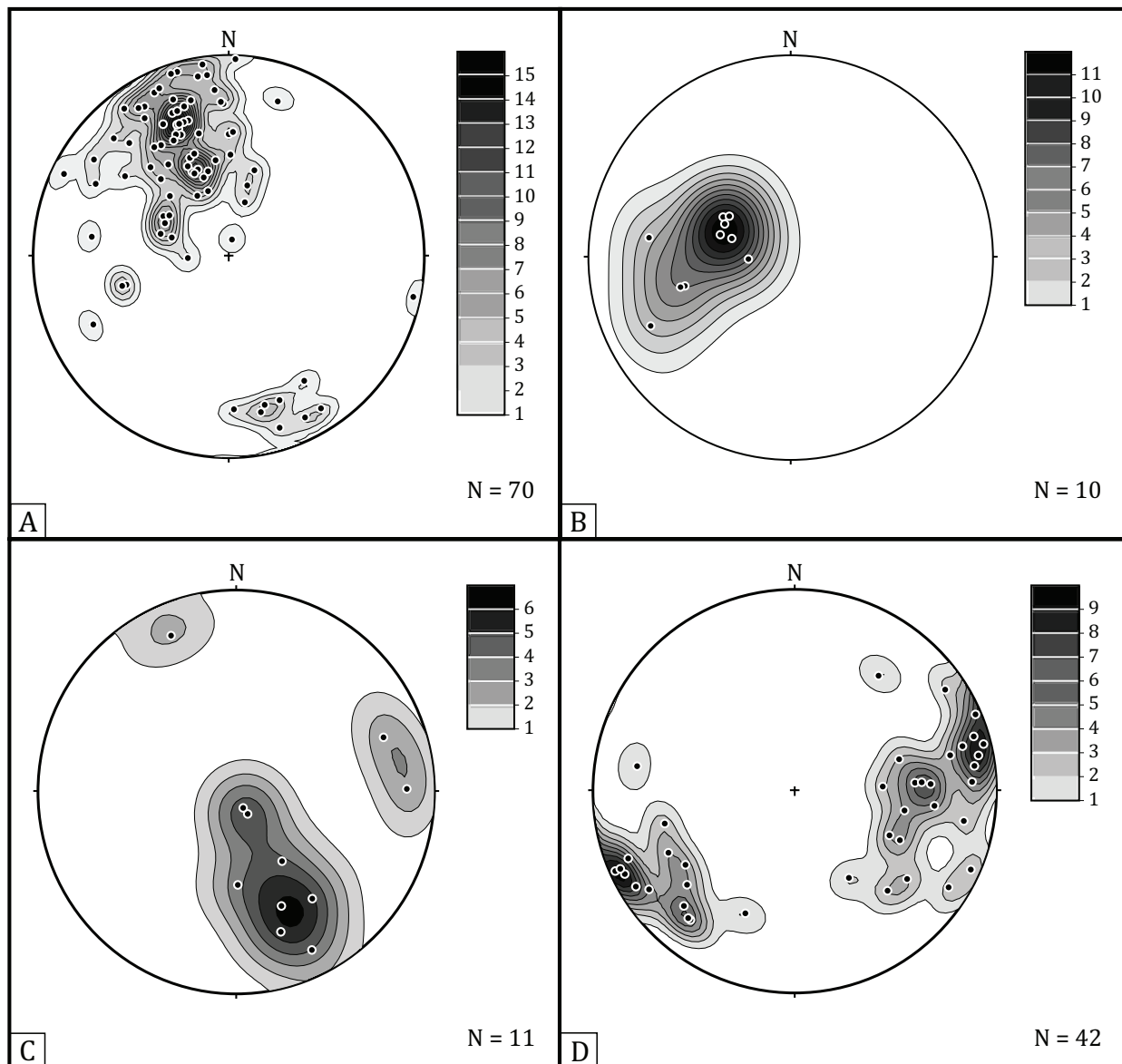


**Fig. 8.** Contour plots of measured Alpine foliations and lineations in the Tatric and Veporic units: **A** — Alpine  $S_1^A$  spaced to mylonitic foliations with asymmetries pointing top-to-the-NNW transport of the Veporic Unit onto the Tatric Unit (poles of planes); **B** — Alpine  $S_2^A$  extensional spaced mylonitic foliation (poles of planes); **C** — Alpine  $L_{1f}^A$  mineral and stretching lineations indicating top-to-the-NNW transport of the Veporic Unit onto the Tatric Unit; **D** — Alpine  $L_{1c}^A$  crenulation and intersection lineations perpendicular to the Eo-Alpine transport direction.

generally displaced from north to south. In contrast, Alpine tectogenesis had an NNW-vergence and overprinted the former Variscan structure by Alpine processes that complicate the structure of the area. The  $D_1^A$  deformation was accompanied by retrograde metamorphism only at sites of extreme influence and suitable petrographic composition of the deformed rock.  $P$ - $T$  conditions were lower during  $D_1^A$  deformation than in the case of  $D_1^V$  or  $D_2^V$  deformations. More pronounced flow (ductile) structures with complete transposition of older structures into younger ones ( $S_1^A$ ) occurred only locally, especially along the reverse shear zones with top-to-the-NNW movement. The vergency of Alpine reverse shear zones,

mainly along the Čertovica shear zone, is also documented by stretching and mineral lineations ( $L_{1f}^A$ ) on newly formed shear planes ( $S_1^A$ ) developed during the simple shear regime with well-developed  $S$ - $C$  fabric. The NNW-SSE shortening was also revealed by the attitude of the  $F_1^A$  folds and  $L_{1c}^A$  intersection and crenulation lineations (Fig. 8C,D). Alpine deformation and kinematics were first documented in detail in the work of Siegl (1976a, 1981) and is consistent with our observations. The  $D_1^A$  is related to the Alpine thrusting of the Veporic Unit onto the Tatric Unit during the Eo-Alpine nappe formation (90–70 Ma) (cf. Putiš 1992; Putiš et al. 2009).

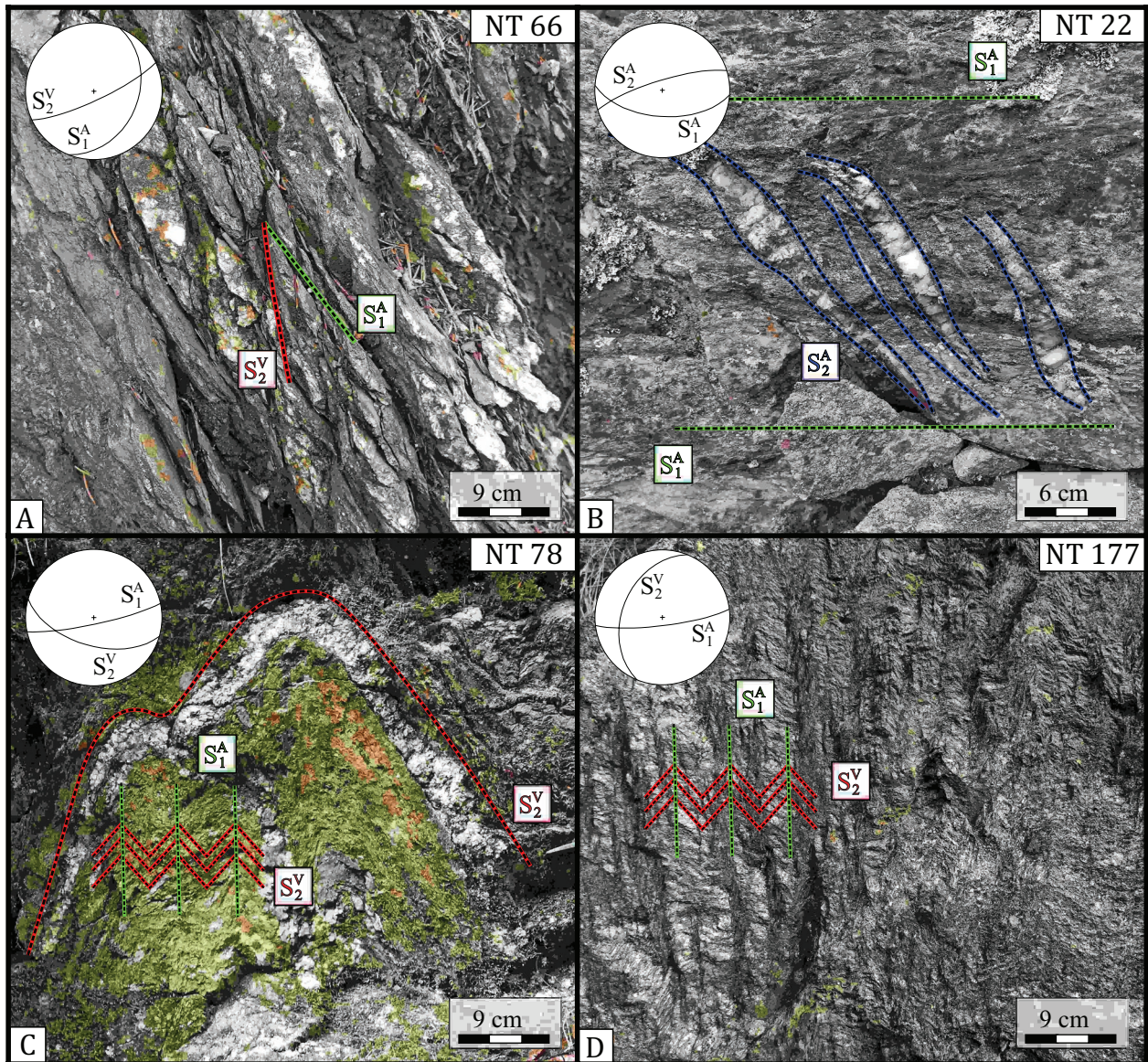


**Fig. 9.** Field photographs of the Alpine fabric: **A** — Pervasive Variscan  $S_2^V$  foliation overprinted by Alpine mylonitic foliation ( $S_1^A$ ) in Paleozoic paragneiss (Veporic crystalline basement); **B** — En-echelon quartz veins in Lower Triassic sandstone (Tatric cover sequence); **C** — Folded pegmatite vein in deformed orthogneiss (folded  $S_2^V$  foliation) with pronounced crenulation cleavage ( $S_1^A$ ); **D** — Alpine crenulation cleavage ( $S_1^A$ ) in Paleozoic paragneiss (Jarabá Complex, Tatric Unit), formed during late Cretaceous shortening.

In the metamorphosed rocks of the Jarabá Complex of the Tatric Unit and the northern Veporic Unit, folds ( $F_1^A$ ) of different amplitude and wavelength are presented, which are genetically distinct from the Variscan  $F_1^A$  and  $F_2^V$  folds. Their attitude is the same as the attitude of the Variscan folds (E–W to NE–SW striking of fold hinges), however, the inclination of their axial planes is mainly steep to the south and less to the north. Moreover, the inclination of fold axial planes ( $F_1^A$ ) to the southeast is progressively becoming shallower. In addition, the fold asymmetry increases in a south-eastward direction, especially in the broader area along the Čertovica shear zone. The folds ( $F_1^A$ ) were more frequently observed in paragneisses and the Mesozoic rock of the cover sequences.

In many places, Mesozoic sedimentary tectonic lenses are folded along the mylonite zones and thus incorporated into the crystalline basement. The relatively-varied types of folds ( $F_1^A$ ) are conditioned by the rheology of the rocks, the low degree of Alpine metamorphism, and the pronounced planar predisposition of the rocks with pervasive  $S_2^V$  fabric.

## Conclusions

Two main deformation groups were distinguished by structural research. The older group of deformations ( $D^V$ ) is related to the Variscan higher-grade metamorphism and the younger

deformations group ( $D^A$ ) is characterised by the deformation of low-grade (retrograde) metamorphism.

Variscan deformation can be divided into three phases. The  $D_1^V$  deformation is only sporadically recognizable in low-strain domains and is characterized by tight, isoclinal, and sheath folds ( $F_2^V$ ) that fold limbs ( $S_1^V$ ), which are conformable with the  $S_2^V$  foliation – clearly confirming its oldest age. The fold axes ( $F_2^V$ ) have a large spatial variance, but in general, they are E–W oriented. We can exclude that the deformation ( $D_1^V$ ) may also be pre-Variscan.

Deformation ( $D_2^V$ ) was accompanied by progressive metamorphism and granitization, and is the most complex and significant process producing pervasive metamorphic foliation ( $S_2^V$ ) throughout the study area. The foliation ( $S_2^V$ ) determines the anisotropy of the majority of observed metamorphosed rocks. Mineral and stretching lineations ( $L_{2r}^V$ ) oriented in an ENE–WSW direction are also associated with the deformation ( $D_2^V$ ), but are not as pervasive as foliations ( $S_2^V$ ).

The  $S_2^V$  foliation is folded by non-penetrative folds ( $F_2^V$ ) with the trend of fold axes ( $F_2^V$ ) in an E–W direction. The new fabric is represented by non-penetrative cleavage ( $S_3^V$ ), as well as by intersection and crenulation lineations ( $L_{3c}^V$ ). The last observed Variscan deformation ( $D_4^V$ ) is accompanied by the aplites, pegmatites, or quartz veins ( $S_4^V$ ), which are predominantly in two directions –  $S_2^V \parallel S_4^V$  and  $S_2^V \perp S_4^V$  and linear structures were observed.

The Alpine deformation ( $D_1^A$ ) was accompanied by retrograde metamorphism and the evolution of deformation fabric is more significantly localized to shear zones and evolved during the Cretaceous orogeny (Eo-Alpine deformation). The  $p$ – $T$  conditions for metamorphism were lower in the case of deformation ( $D_1^A$ ) than in deformation ( $D_2^V$ ), and complete transposition of  $S_2^V$  fabric to the  $S_1^A$  originated only very locally. The deformation ( $D_1^A$ ) is characterized by the evolution of crenulation cleavage that transitions to mylonitic foliation ( $S_1^A$ ) in shear zones. The foliation ( $S_1^A$ ) has average NE–SW striking and inclines shallowly or moderately to the SE in direction. The deformation ( $D_1^A$ ) is also accompanied by NE–SW intersectional lineations ( $L_{1c}^A$ ) and folds ( $F_1^A$ ) that are often asymmetric. The  $L_{1c}^A$  and  $F_1^A$  structures are younger and conformably superimposed on  $L_{2r}^V$  and  $F_2^V$  structures. From these observations, we can unambiguously determine the kinematics of the Alpine thrust deformation with top-to-the-NNW vergency.

The last identified Alpine deformational stage ( $D_2^A$ ) is related to the extensional tectonic regime, especially in the Čertovica shear zone. Extensional structures, such as en-echelon veins ( $S_2^A$ ) and stretching lineation ( $L_{2r}^A$ ) refer to top-to-the-east transport with the orientation of the principal minimal paleo-stress axis in an E–W direction. The  $D_2^A$  structures are not pervasive and were observed mainly in the Lower Triassic metaquartzite and crystalline basement around the Čertovica shear zone.

**Acknowledgements:** This work was supported by the Slovak Research and Development Agency under contracts Nos.

APVV-21-0281 “Alpine geodynamical evolution of the Western Carpathian inner zones”, APVV-17-0170 “Early Alpidic tectonic evolution and palaeogeography of the Western Carpathians” and the VEGA Grant No. 1/0346/20. Ondrej Lexa and Roman Farkašovský are thanked for their constructive reviews, which helped improve this article.

## References

- Allmendinger R.W., Cardozo N. & Fisher D. 2012: Structural geology algorithms: Vectors and tensors in structural geology. *Cambridge University Press*, Cambridge, New York, 1–289.
- Andrusov D., Bystrický J. & Fusán O. 1973: Outline of the Structure of the West Carpathians. X. Congress of Carpathian-Balkan Association. *Geol. Úst. D. Štúra, Vyd. Slov. Akad. Vied*, Bratislava, 1–44.
- Bagdasarjan G.P., Gukasjan R.Kh., Cambel B. & Veselský J. 1985: Rb–Sr isochron dating of the Ďumbier zone granitoids of the Nízke Tatry Mts. (Western Carpathians). *Geologický Zborník Geologica Carpathica* 36, 637–645.
- Bezák V. 1994: Proposal of the new dividing of the West Carpathian crystalline based on the Hercynian tectonic building reconstruction. *Mineralia Slovaca* 26, 1–6 (in Slovak with English abstract and summary).
- Bezák V. & Olšavský M. 2008: Large overthrusts in the Northern Veporicum (Western Carpathians). *Mineralia Slovaca* 40, 121–126 (in Slovak with English abstract and summary).
- Bezák V., Jacko S., Janák M., Ledru P., Petrik I. & Vozárová A. 1997: Main Hercynian lithotectonic units of the Western Carpathians. In: Grecula P., Hovorka D. & Putiš M. (Eds.): Geological Evolution of the Western Carpathians. *Mineralia Slovaca – Monographs*, Bratislava, 261–268.
- Bezák V., Broska I., Ivanička J., Reichwalder P., Vozár J., Polák M., Havrila M., Mello J., Biely A., Plašienka D., Potfaj M., Konečný V., Lexa J., Kaličiak M., Žec B., Vass D., Elečko M., Janočko J., Pereszlényi M., Marko F., Maglay J. & Pristaš J. 2004: Tectonic Map of Slovak Republic. *MŽP SR – ŠGÚDŠ*, Bratislava.
- Biely A., Bezák V., Elečko M., Kaličiak M., Konečný V., Lexa J., Mello J., Nemčok J., Potfaj M., Rakús M., Vass D., Vozár J. & Vozárová A. 1996: Geological map of Slovakia. *Ministerstvo životného prostredia SR, Geologická služba SR*, Bratislava.
- Bojko A., Kamenický L., Semenenko N.P., Cambel B. & Ščerbak N. 1974: Chasť rezul'tatov opredeleniya absol'yutnogo vozrasta gornych porod kristallicheskogo massiva Zapadnykh Karpat i sovremennoye sostoyaniye znaniy. *Geologica Carpathica* 25, 25–38.
- Broska I., Petrik I., Be'eri-Shlevin Y., Majka J. & Bezák V. 2013: Devonian/Mississippian I-type granitoids in the Western Carpathians: A subduction-related hybrid magmatism. *Lithos* 162–163, 27–36. <https://doi.org/10.1016/j.lithos.2012.12.014>
- Burda J., Klötzli U., Woskowicz-Ślęzak B., Li Q.-L. & Liu Y. 2020: Inherited or not inherited: Complexities in dating the atypical ‘cold’ Chopok granite (Nízke Tatry Mountains, Slovakia). *Gondwana Research* 87, 138–161. <https://doi.org/10.1016/j.gr.2020.05.018>
- Cambel B., Král J. & Burchart J. 1990: Izotopová geochronológia kryštalinika Západných Karpát. *VEDA, Slovak Academy of Sciences*, 1–183.
- Cardozo N. & Allmendinger R.W. 2013: Spherical projections with OSXStereonet. *Computers & Geosciences* 51, 193–205. <https://doi.org/10.1016/j.cageo.2012.07.021>

- Fritz H., Neubauer F., Janák M. & Putiš M. 1992: Variscan mid-crustal thrusting in the Carpathians. Part II: Kinematics and fabric evolution of the Western Tatra basement. *Terra Abstract Supplement* 2, 24.
- Froitzheim N., Plašienka D. & Schuster R. 2008: Alpine tectonics of the Alps and Western Carpathians. In: McCann T. (Ed.): *The geology of Central Europe*. Vol. 2, Mesozoic and Cenozoic. *Geol. Soc. Publ. House*, London 1141–1232.
- Hók J., Šujan M. & Šipka F. 2014: Tectonic division of the Western Carpathians: an overview and a new approach. *Acta Geologica Slovaca* 6 135–143 (in Slovak with English summary).
- Janák M., Plašienka D., Frey M., Cosca M., Schmidt S.Th., Lupták B. & Méres Š. 2001: Cretaceous evolution of a metamorphic core complex, the Veporic unit, Western Carpathians (Slovakia): P–T conditions and in situ  $^{40}\text{Ar}/^{39}\text{Ar}$  UV laser probe dating of metapelites. *Journal of Metamorphic Geology* 19, 197–216. <https://doi.org/10.1046/j.0263-4929.2000.00304.x>
- Jeřábek P., Janák M., Faryad S.W., Finger F. & Konečný P. 2008: Polymetamorphic evolution of pelitic schists and evidence for Permian low-pressure metamorphism in the Vepor Unit, West Carpathians. *Journal of Metamorphic Geology* 26, 465–485. <https://doi.org/10.1111/j.1525-1314.2008.00771.x>
- Kamb W.B. 1959: Ice petrofabric observations from Blue Glacier, Washington in relation to theory and experiment. *Journal of Geophysical Research* 64, 1891–1909.
- Kantor J. 1959: Príspevok ku geochronológii nízkotatranských granitoidov. *Geologické Práce, Zošit* 55, 159–169.
- Kantor J. 1961: Beitrag Zur Geochronologie der Magmatite und Metamorfite des westkarpathischen Kristallins. *Geologické Práce, Správy* 60, 303–317.
- Kohút M. & Larionov A.N. 2021: From subduction to collision: Genesis of the Variscan granitic rocks from the Tatric Superunit (Western Carpathians, Slovakia). *Geologica Carpathica* 72, 96–113. <https://doi.org/10.31577/GeolCarp.72.2.2>
- Krist E., Korikovskij S.P., Putiš M., Janák M. & Faryad S.W. 1992: Geology and Petrology of metamorphic rocks of the Western Carpathian crystalline complexes. *Comenius University Press*, Bratislava, 1–324.
- Kubíny D. 1956: Zpráva o výskume ústrednej časti d'umbierskeho masivu. *Geologické Práce, Zprávy* 9, 110–117.
- Kubíny D. 1958: Predbežné výsledky z geologického mapovania nízkotatranského granitoidného masivu. *Geol. Práce, Zprávy* 14, 129–133.
- Kubíny D. 1960: Príspevok ku geológii okolia Trangošky. *Geologické Práce, Zprávy* 17, 97–104.
- Lisle R.J. & Leyshon P.R. 2004: Stereographic Projection Techniques for Geologists and Civil Engineers. 2<sup>nd</sup> edition, *Cambridge University Press*, Cambridge, 1–112.
- Madarás J., Putiš M. & Hók J. 1999: Structural features of the Hercynian tectonics in the southern part of the Ďumbier crystalline complex (Low Tatra Mts., Western Carpathians). *Mineralia Slovaca* 31, 17–30 (in Slovak with English summary).
- Mahel M., Kamenický J., Fusán O. & Matějka A. 1968: Regional geology of Czechoslovakia, Part II, the Western Carpathians. Geological Survey of Czechoslovakia in Academia, Praha, 1–707.
- Maraszewska M., Broska I., Kohút M., Yi K., Konečný P. & Kurylo S. 2022: The Ďumbier–Prášivá high K calc-alkaline granite suite (Low Tatra Mts., Western Carpathians): Insights into their evolution from geochemistry and geochronology. *Geologica Carpathica* 73, 273–291. <https://doi.org/10.31577/GeolCarp.73.4.1>
- Matějka A. & Andrusov D. 1931: Aperçu de la géologie des Carpathes occidentales de la Slovaquie central et des régions avoisinantes. *Knih. SGÚ* 13A, 19–163.
- Mišík M., Chlupáč I. & Cicha I. 1985: Stratigraphical and historical geology. *SPN*, Bratislava, 1–570.
- Petrík I., Konečný P., Kováčik M. & Holický I. 2006: Electron microprobe dating of monazite from the Nízke Tatry Mountains orthogneisses (Western Carpathians, Slovakia). *Geologica Carpathica* 57, 227–242.
- Plašienka D. 1999: Tectochronology and paleotectonic model of the Jurassic–Cretaceous evolution of the Central Western Carpathians. *Veda, SAV*, Bratislava, 1–125.
- Plašienka D. 2018: Continuity and episodicity in the Early Alpine tectonic evolution of the Western Carpathians: how large-scale processes are expressed by the orogenic architecture and rock record data. *Tectonics* 37, 2029–2079. <https://doi.org/10.1029/2017TC004779>
- Putiš M. 1992: Variscan and Alpidic nappe structures of the Western Carpathian crystalline basement. *Geologica Carpathica* 43, 369–380.
- Putiš M., Filová I., Korikovskij S.P., Kotov A.B. & Madarás J. 1997: Layered metaigneous complex of the Veporic basement with features of the Variscan and Alpine thrust tectonics (the Western Carpathians). In: Grecula P., Hovorka D. & Putiš M. (Eds.): *Geological Evolution of the Western Carpathians. Mineralia Slovaca – Monographs*, Bratislava, 176–196.
- Putiš M., Kotov A.B., Petrik I., Korikovskij S.P., Madarás J., Salmikova E.B., Yakovleva S.Z., Berezhnaya N.G., Plotkina Y.V., Kovach V.P., Lupták B. & Majdán M. 2003: Early- vs. Late orogenic granulite relationships in the Variscan basement of the Western Carpathians. *Geologica Carpathica* 54, 163–174.
- Putiš M., Sergeev S., Ondrejka M., Larionov A., Siman P., Spišiak J., Uher P. & Paderin I. 2008: Cambrian-Ordovician metaigneous rocks associated with Cadomian fragments in the West-Carpathian basement dated by SHRIMP on zircons: a record from the Gondwana active margin setting. *Geologica Carpathica* 59, 3–18.
- Putiš M., Frank W., Plašienka D., Siman P., Sulák M. & Biroň A. 2009: Progradation of the Alpidic Central Western Carpathians orogenic wedge related to two subductions: constrained by  $^{40}\text{Ar}/^{39}\text{Ar}$  ages of white micas. *Geodynamica Acta* 22, 31–56.
- Ramsay J.G. & Huber M.I. 1987: The Techniques of Modern Structural Geology, Vol. 2: Folds and Fractures. *Pergamon Press*, London.
- Siegl K. 1967: Predbežné výsledky štúdia tektoniky kryštalinika veporid a tatrid medzi Sihlou a Ďumbierom. *Acta Geologica et Geographica Universitatis Comenianae, Geologia* 12, 105–114.
- Siegl K. 1970: Fabric anisotropy of Ďumbier granodiorite. *Geologický Zborník Geologica Carpathica* 21, 327–334.
- Siegl K. 1973: The fabric of mesoscopic folds of different structural regimes from metamorphites of the western part of Low Tatra Mts. (West Carpathians). *Geologický Zborník Geologica Carpathica* 24, 205–222.
- Siegl K. 1976a: Vrásové deformácie d'umbierskeho kryštalinika [Fold deformation of the Ďumbier crystalline basement]. *Acta Geologica et Geographica Universitatis Comenianae, Geologia* 28, 115–125.
- Siegl K. 1976b: The structure of the Low Tatra pluton (West Carpathians). *Geologický Zborník – Geologica Carpathica* 27, 149–164.
- Siegl K. 1981: Structure of the Ďumbier metamorphites (West Carpathians). *Geologický Zborník – Geologica Carpathica* 32, 113–127.
- Zoubek V. 1936: Poznámky o krystaliniku Západných Karpát. *Věstník SGÚ* 12, 6.
- Zoubek V. 1951: Zpráva o geologickém výskumu jižního svahu N. Tatier medzi Bystrou a Jasenskou dolinou. *Věstník ÚÚG* 26, 162–166.